

# New molecular materials for hole injection: the synthesis and *in situ* ESR-UV/Vis/NIR spectroelectrochemistry of 2-diarylaminothiophene-based starburst compounds

Peter Rapta,<sup>ab</sup> Ahacene Tabet,<sup>c</sup> Horst Hartmann<sup>c</sup> and Lothar Dunsch<sup>\*a</sup>

Received 24th July 2007, Accepted 2nd October 2007

First published as an Advance Article on the web 19th October 2007

DOI: 10.1039/b711328e

A series of 2-diarylaminothiophene-based starburst compounds **14–16** with a central triphenylamino-, benzene-, and 1,3,5-triphenylbenzene moiety, respectively, were prepared at moderate yields by a palladium-catalysed coupling reaction. Their electrochemical, optical and magnetic properties were studied with respect to their application as hole transport materials, using cyclic voltammetry and *in situ* ESR-UV/Vis/NIR spectroelectrochemistry. Although all prepared 2-diarylaminothiophene-based starburst compounds are structurally related, their electrochemical properties differ in their dependence on the central moiety. The number of reversible voltammetric peaks is diminished upon changing the central triphenylamino moiety of the starburst compounds to a central benzene or 1,3,5-triphenylbenzene moiety. The simultaneous multiple electron transfer as well as the location of the spins on the core moieties was detected in the oxidation of the 1,3,5-triphenylbenzene based starburst compound. The stability of the charged states increased substantially upon the incorporation of a thiophene moiety between the central moieties and the side groups.

## Introduction

Organic  $\pi$ -conjugated compounds which exhibit a good glass-forming tendency, accompanied by a pronounced facility to be transformed into charged species by their oxidation, have received a lot of interest in recent years. Among these compounds triphenylamine **1** and several of its derivatives (Scheme 1), such as the benzidine compound **2** (TPD) and the starburst compounds **3** (DATA) and **4** (TDAPB), play a crucial role in the search for new materials in different applications<sup>1</sup> like charge transport materials for several types of optoelectronic devices, such as organic light-emitting diodes, organic solar cells, and data storage devices.<sup>2</sup> In common, they can be easily prepared by a heavy-metal catalysed C,N- or C,C-coupling reaction<sup>3</sup> starting from suitable building blocks.

Recently it was demonstrated that 2-diarylaminothiophenes **5** as heterocyclic triarylamine analogues have similar properties to the triarylamines themselves. Thus, 2-diarylaminothiophenes are able to vitrify very easily and to form stabilised radical cations and dications by oxidation.<sup>4</sup> Due to these properties 2-diarylaminothiophenes were used as building blocks for preparing compounds with promising charge transport properties. For instance, the compounds **6<sub>n</sub>–8** are

such candidates (Scheme 1). They have been prepared from the parent 2-diphenylaminothiophene **5a** (Scheme 2) by an oxidative dimerisation<sup>5</sup> (for **6<sub>0</sub>**) or by a palladium- or copper-catalysed coupling reaction with dibromo(het)arylenes,<sup>6</sup> 4,4',4''-tribromobenzene<sup>7</sup> and hexabromobenzene.<sup>8</sup> They are claimed to be promising hole transport materials.<sup>9</sup> We have used the parent 2-diphenylaminothiophene **5a** and the derivatives **5b** and **5c** as educts for preparing the heterocyclic analogues **14–16** of the above-mentioned carbocyclic starburst compounds **3** and **4** and studied their electrochemical properties with respect to their application as hole transport materials. Besides the electrochemical characterisation the charged states in the compounds were studied by *in situ* UV/VIS/NIR and ESR spectroscopy.

## Results and discussion

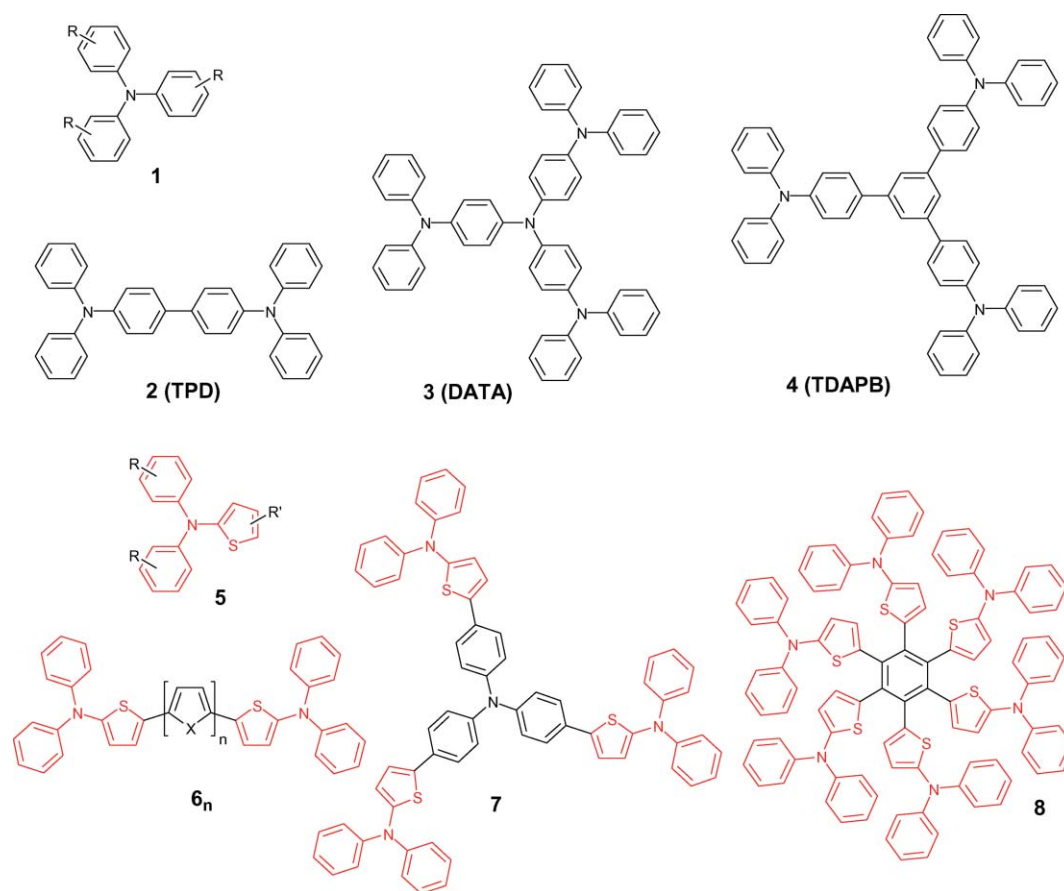
### Synthesis and characterization of 2-diarylaminothiophene based starburst compounds 14–16

The synthesis of starburst compounds with 2-diarylaminothiophene moieties follows the routes for preparing 2-diaryl-amino-substituted oligothiophenes such as the  $\alpha,\omega$ -bis(diphenylamino)-substituted oligothiophenes **6**.<sup>8</sup> It starts with the transformation of the 2-diarylaminothiophenes **5a–5c** into their metallated species **9a–9c** and **10a–10c** and ends up in a palladium-catalysed C,C-coupling reaction of the tributylstannyl compounds **10a–10c** with the tribromo compounds **11–13** (Scheme 2). Thus, the starburst-like compounds **14a–14c**, **15a–15c**, and **16a–16c** can be prepared in moderate yields. The synthesis of the starting compounds **5a–5c** has been published previously.<sup>6</sup> It consists of a heterocyclisation procedure starting from acyclic 1-chlorotrimethinium salts

<sup>a</sup>IFW Dresden, Leibniz-Institute of Solid State Research, Department of Electrochemistry and Conducting Polymers, Helmholtzstrasse 20, D-01069 Dresden, Germany

<sup>b</sup>Slovak University of Technology, Faculty of Chemical and Food Technology, Department of Physical Chemistry, Radlinského 9, SK-812 37 Bratislava, Slovak Republic

<sup>c</sup>University of Technology Dresden, Institute of Applied Photophysics, D-01062 Dresden, Germany



Scheme 1

which react with alkylthioglycolates giving rise to the formation of 2-diarylamino-substituted alkyl thiophene-5-carboxylates<sup>10</sup> from which the desired 2-diphenylaminothiophenes **5** have been prepared by saponification and subsequent decarboxylation of the 2-aminothiophene-5-carboxylic acids primarily formed.

The structures of the prepared starburst compounds **14–16** which are, apart from compounds **14a**<sup>7</sup> and **15a**,<sup>11</sup> unknown till now, were confirmed by elemental analyses, mass spectra, and NMR data. Thus, all of these 2-amino-5-thienyl starburst compounds exhibit in their mass spectra an intense molecular ion peak. The <sup>1</sup>H NMR spectra of the compounds **14–16** give characteristic signals at about 6.7–6.8 and 7.6–7.8 ppm. These signals are not hidden under the signals of the protons at the *N*-aryl moieties and appear as doublets or singlets. They can be unambiguously attributed to the protons at the thiophene ring and, for compounds **15** and **16**, to the central benzene moieties.

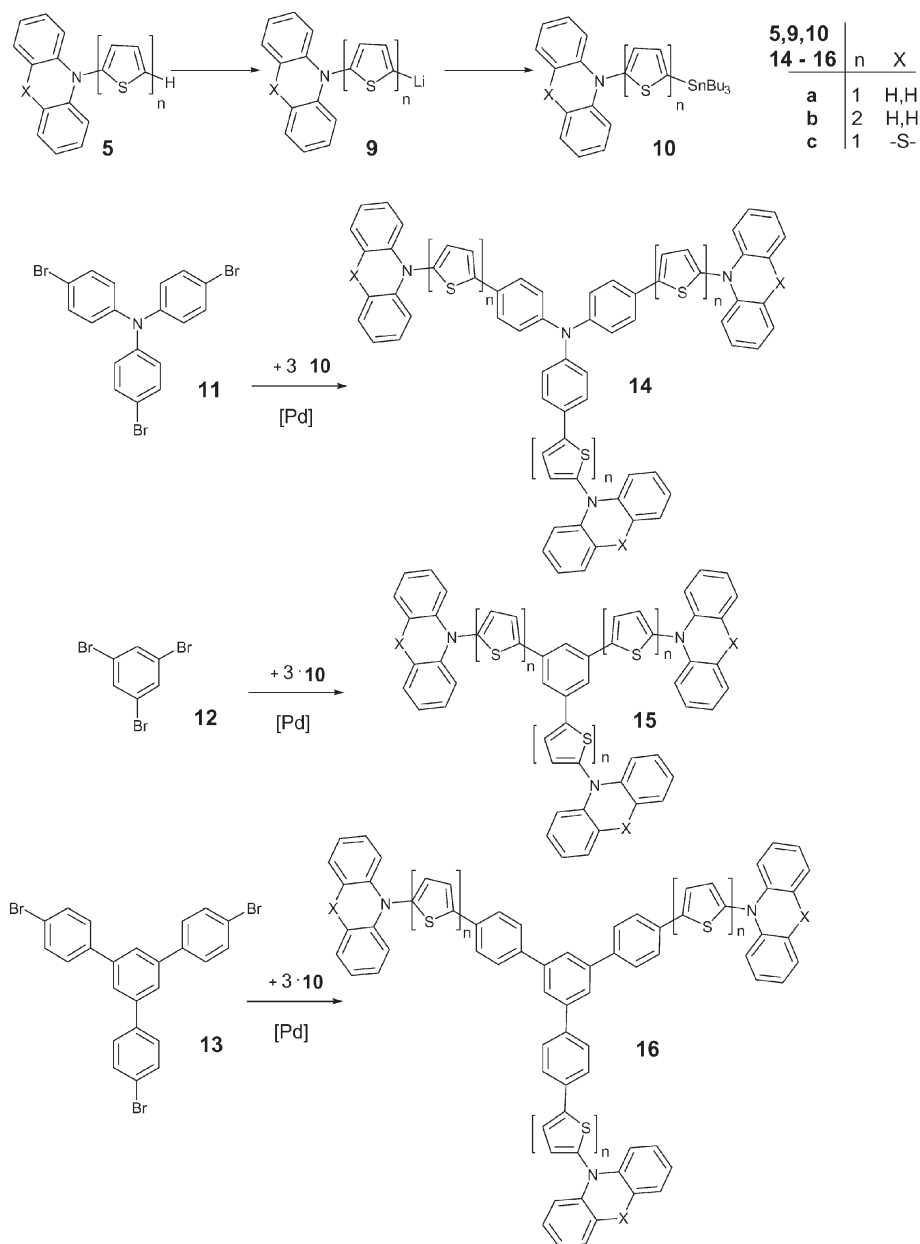
As expected, some of the starburst compounds prepared exhibit a high tendency to form amorphous glasses after cooling their melts. These properties were checked by DSC measurements. The compounds **15a**, **15b**, and **15c** exhibit a glass transition at 82 °C, 100 °C, and 88 °C, respectively, in a second heating of their cooled melts.

### Spectroelectrochemistry

Although all the 2-diarylaminothiophene-based starburst compounds **14–16** are structurally related, their electrochemical

properties differ to a certain extent. Similar electrochemical properties were observed for the triphenylamine-based compounds, measured in dichloromethane containing tetrabutylammonium tetrafluoroborate (TBABF<sub>4</sub>) as supporting electrolyte, four reversible one-electron processes during oxidation at a scan rate of 0.1 V s<sup>-1</sup> are recorded. For compound **14a**, the half-wave potentials  $E_{1/2}$  vs. ferrocene/ferrocenium redox couple (Fc/Fc<sup>+</sup>) were evaluated to be 0.07, 0.18, 0.35 and 0.54 V, respectively (see Fig. 1a and Table 1). Remarkably, the peak separation  $\Delta E$  between neighbouring voltammetric peaks increases with the number of electrons transferred from 0.11 V ( $E_{1/2}^2 - E_{1/2}^1$ ) to 0.19 V ( $E_{1/2}^4 - E_{1/2}^3$ ) indicating a strong charge delocalisation in this molecule.

During the *in situ* study of the oxidation of **14a** by ESR-UV/Vis/NIR spectroelectrochemistry at a platinum mesh electrode (scan rate  $\nu = 3$  mV s<sup>-1</sup>) two optical transitions arise at 2.19 eV (566 nm) and 0.98 eV (1265 nm) at the electrode potential of the first electron transfer (Fig. 2a). Simultaneously, broad unresolved ESR spectra with a *g*-value of 2.0027 were observed (Fig. 2b). The shape of ESR spectrum indicates the presence of a large set of unresolved splittings by the central triphenylamine moiety of the molecule.<sup>12</sup> This assumption was confirmed by the spectroelectrochemical investigation of **14c** and **14b** under the same experimental conditions. In **14c** the diphenylamino



Scheme 2

moiety of **14a** is replaced by a phenothiazinyl moiety and in **14b** an additional thiophene moiety is inserted into the bridge between the central triphenylamine and the 2-aminothiophene fragments. Similarly to the oxidation of **14a**, the cyclic voltammetry of a solution of **14c** gives four reversible one-electron processes at a scan rate of  $0.1 \text{ V s}^{-1}$  (Fig. 1b, Table 1). However, the peak separation  $\Delta E$  is much smaller than for **14a**. The first and the second voltammetric peak are coincident and the third and fourth electron transfer reactions proceed at higher potentials. In the first oxidation step of **14c** very similar optical transitions (at  $2.19 \text{ eV}$  ( $566 \text{ nm}$ ) and  $1.07 \text{ eV}$  ( $1159 \text{ nm}$ )) (Fig. 2c) were observed and identical ESR spectra (see broad ESR lines at  $g = 2.0027$  in Fig. 2d) as compared to the detected cation radical of **14a**. These observations confirm a spin delocalisation on the central

triphenylamino moiety in the monocation of **14c** which is the same as in compound **14a**.

By increasing the electrode potential to the value of the second electron transfer a slight shift of low optical energy transitions was observed only for both compounds **14a** and **14c** (see transitions at  $\sim 0.97 \text{ eV}$  ( $1278 \text{ nm}$ ) in Fig. 2a and at  $1.04 \text{ eV}$  ( $1192 \text{ nm}$ ) in Fig. 2c). At the electrode potentials of the third and the fourth electron transfer significant changes in the optical as well as the ESR spectra were observed for **14c**. Here, new absorptions arise at  $2.37 \text{ eV}$  ( $523 \text{ nm}$ ) and  $1.68 \text{ eV}$  ( $738 \text{ nm}$ ). Simultaneously, intense ESR spectra with strongly shifted  $g$ -values ( $g = 2.0056$ ) were observed. The ESR spectra change their shape going from the third to the fourth oxidation peak (Fig. 2d). In the potential region of the third oxidation peak a line broadened ESR spectrum with a dominant ESR

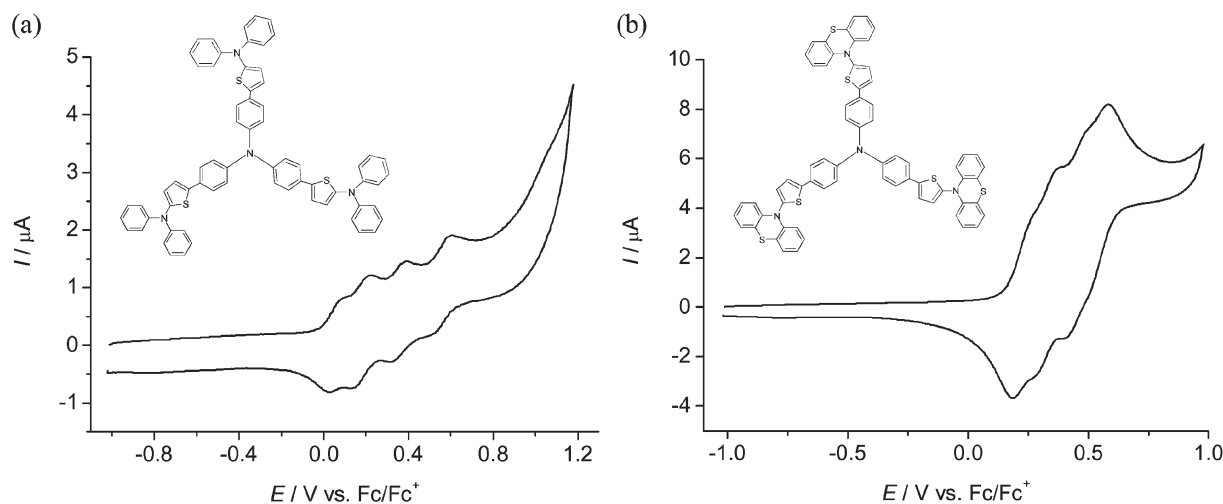


**Fig. 1** Cyclic voltammograms of  $1 \times 10^{-3} \text{ mol L}^{-1}$  (a) **14a** and (b) **14c** in  $\text{CH}_2\text{Cl}_2 + 0.1 \text{ mol L}^{-1} \text{ TBABF}_4$  at a platinum wire electrode (scan rate:  $\nu = 100 \text{ mV s}^{-1}$ ).

splitting constant caused by one nitrogen atom with  $a_N = 0.58 \text{ mT}$  was observed (see ESR spectrum at  $0.6 \text{ V}$  in Fig. 2d). A number of neighbouring hydrogen nuclei having different hyperfine coupling constants cause strong line broadening. The high  $g$ -value as well as the shape of ESR signal point to the localisation of the additional charge and spin on the phenothiazinyl moiety. Consequently, new optical transitions are observed at the third and fourth electron transfer stages. They can be attributed to the charged phenothiazinyl moiety in which significant charge localisation obviously occurs. The ESR spectra observed in the region of the fourth electron transfer (see ESR spectrum at  $0.9 \text{ V}$  in Fig. 2d) can be simulated with two equivalent nitrogen splitting constants  $2a_N = 0.3 \text{ mT}$  confirming the charging of the further phenothiazinyl moiety and indicating strong electronic coupling between the charged arm moieties.

The number of reversible voltammetric peaks is diminished for the starburst compounds **16** with the central 1,3,5-triphenylbenzene moiety. Thus, for compounds **16a** and **16c** only one reversible oxidation peak is observed at  $E_{1/2} = 0.32 \text{ V}$  and  $E_{1/2} = 0.40 \text{ V}$  vs.  $\text{Fc/Fc}^+$ , respectively. Comparing the peak currents of these structures in their cyclic voltammograms with

that of ferrocene at the same concentration the height of the ferrocene peak was approximately 3 times smaller than that of the peaks of **16a** and **16c**. Therefore, three strongly overlapping one electron processes are proposed at this potential for both starburst compounds **16a** and **16c**. The *in situ* spectroelectrochemical study of the oxidation of **16c** at the first voltammetric peak (Fig. 3a, scan rate  $\nu = 3 \text{ mV s}^{-1}$ ) gives the same ESR spectra (see inset in Fig. 3b) as for the oxidation of **14c** at electrode potentials of the third electron transfer. Simultaneously well defined optical transitions were observed at  $2.56 \text{ eV}$  ( $484 \text{ nm}$ ),  $1.77 \text{ eV}$  ( $701 \text{ nm}$ ), and  $1.50 \text{ eV}$  ( $827 \text{ nm}$ ), respectively (Fig. 3b). By increasing the electrode potential line broadened ESR spectra were observed indicating a strong interaction of spins. Such an effect is well known for biradicals and triradicals formed during the oxidation of structures where a dipolar coupling of the electron spins strongly broadens the ESR spectra.<sup>12</sup> Similar optical transitions at  $2.54 \text{ eV}$  ( $488 \text{ nm}$ ) and  $1.58 \text{ eV}$  ( $784 \text{ nm}$ ) were observed for the oxidation products of **16a**, where the phenothiazinyl moieties are replaced by a diphenylamino group. Broad unresolved ESR spectra at a  $g$ -value of 2.0027 similar to that of the oxidation products of **14a** were observed in the oxidation of **16a** indicating the localisation of the spin density at the diphenylamino-thiophene arm moieties.

In cyclic voltammetry of compound **14b** some multistep reversible electron transfer processes were observed at a scan rate of  $0.1 \text{ V s}^{-1}$  (Table 1, Fig. 4a). The peak separation for the first two peaks is relatively small ( $\Delta E = 0.15 \text{ V}$ ), while the peak separation of the second and third peaks is large ( $\Delta E = 0.33 \text{ V}$ ). Two new optical transitions arise at  $0.94 \text{ eV}$  ( $1319 \text{ nm}$ ) and  $1.84 \text{ eV}$  ( $674 \text{ nm}$ ) at the electrode potential of the first electron transfer, as measured by *in situ* ESR-UV/VIS/NIR spectroelectrochemistry at a scan rate of  $3 \text{ mV s}^{-1}$  (Fig. 4a). By increasing the potential to that of the second electron transfer the absorption peaks shift to  $0.98 \text{ eV}$  ( $1265 \text{ nm}$ ) and  $2.17 \text{ eV}$  ( $571 \text{ nm}$ ), respectively. For the third redox reaction an absorption peak at  $1.39 \text{ eV}$  ( $892 \text{ nm}$ ) is detected (Fig. 4a). Intense and broad singlet ESR spectra with

**Table 1** Cyclic voltammetry data (in volts vs.  $\text{Fc/Fc}^+$  redox couple) for compounds **14–16** in oxidation ( $\text{CH}_2\text{Cl}_2 + 0.1 \text{ mol L}^{-1} \text{ TBABF}_4$ , platinum working electrode, scan rate  $\nu = 0.1 \text{ V s}^{-1}$ ).  $E_{1/2}^i$  ( $i = 1-4$ ) are the half-wave potentials in volts vs.  $\text{Fc/Fc}^+$  for the corresponding oxidation peaks

Sample	$E_{1/2}^1$	$E_{1/2}^2$	$E_{1/2}^3$	$E_{1/2}^4$
<b>14a</b>	0.07	0.18	0.35	0.54
<b>14b</b>	0.17	0.32	0.65	
<b>14c</b>	0.23	0.33	0.45	0.53
<b>16a</b>	0.32			
<b>16b</b>	0.19	0.49	0.62	
<b>16c</b>	0.40			
<b>15a</b>	0.36 <sup>a</sup>			
<b>15b</b>	0.26			
<b>15c</b>	0.44 <sup>a</sup>			

<sup>a</sup> Follow-up reactions.

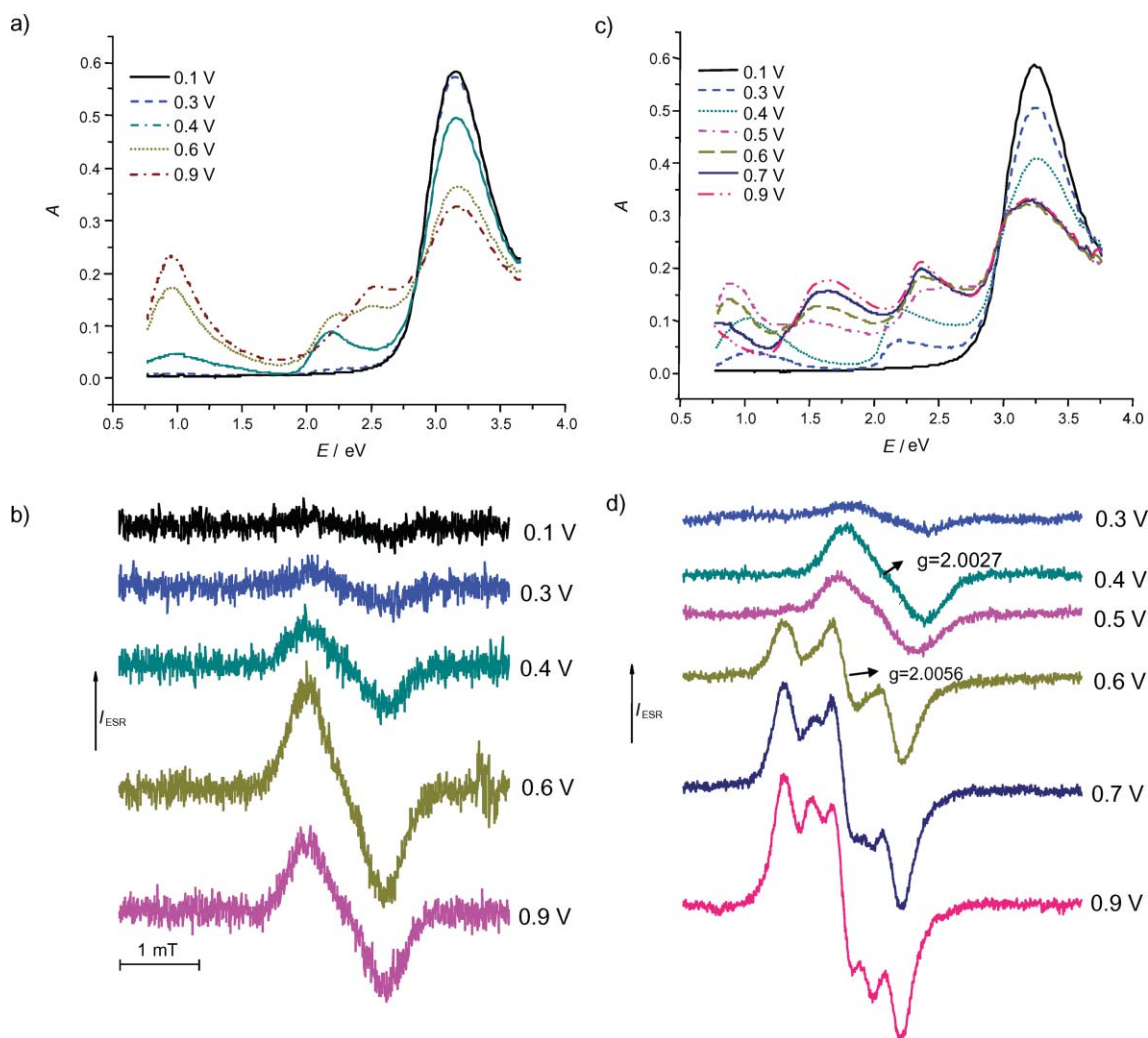


**Fig. 2** UV/Vis/NIR spectra and ESR spectra measured during the oxidation of **14a** (a,b) and **14c** (c,d) in  $0.2 \text{ mol L}^{-1}$  TBABF<sub>4</sub>-CH<sub>2</sub>Cl<sub>2</sub> (platinum mesh working electrode, scan rate  $\nu = 3 \text{ mV s}^{-1}$ ). Identically colored ESR and optical spectra correspond to the potential in volts vs. Fc/Fc<sup>+</sup> marked in the figure with the same trace.

$g \sim 2.003$  and a line width of  $0.7 \text{ mT}$  were observed for the species generated in the first electron transfer.

Similar redox behaviour was observed for the electrochemical oxidation of **16b** (Fig. 4b), in which the conjugated  $\pi$ -system is extended by the insertion of a thiophene moiety between each of the core diphenylamino group and the central 1,3,5-triphenylbenzene moiety. Compound **16b** exhibits reversible voltammetric peaks at  $0.19 \text{ V}$  and  $0.62 \text{ V}$  vs. Fc/Fc<sup>+</sup> (Table 1, Fig. 4b). The species generated in the first oxidation peak gives rise to an absorption maximum at  $1.53 \text{ eV}$  ( $810 \text{ nm}$ ) which shifts under further oxidation to  $1.43 \text{ eV}$  ( $867 \text{ nm}$ ), while a new absorption band arises simultaneously at  $2.12 \text{ eV}$  ( $585 \text{ nm}$ ). The species generated at the second oxidation peak, the potential of which is strongly shifted to higher values, give rise to an absorption maximum at  $1.70 \text{ eV}$  ( $729 \text{ nm}$ ) (Fig. 4b). Negligible ESR intensity is caused by the formation of ESR silent dicationic species.

The starburst compounds **15a–15c** with a central benzene core exhibit different cyclic voltammetric as well as spectroelectrochemical behaviour depending on the number of

thiophene units in the molecule. Broad voltammetric peaks at electrode potentials of about  $0.4 \text{ V}$  vs. Fc/Fc<sup>+</sup> have been detected for compounds **15a**, **15c** and **15b** (Table 1). At this electrode potential a low intensity ESR signal with a rich hyperfine splitting was observed in oxidation of **15a** (Fig. 5a). Simultaneously new absorption peaks at  $1.55 \text{ eV}$  ( $800 \text{ nm}$ ),  $2.36 \text{ eV}$  ( $525 \text{ nm}$ ), and  $2.95 \text{ eV}$  ( $420 \text{ nm}$ ) were detected during the voltammetric scan (Fig. 5a). However the intensity of the most intense absorption peak at  $1.55 \text{ eV}$  ( $800 \text{ nm}$ ) does not correlate with the intensity of the ESR signal simultaneously measured in a voltammetric scan. This new band is slightly shifted to lower energies compared to the cation radical band ( $1.69 \text{ eV}$ ) ( $734 \text{ nm}$ ) and decreases during the back scan (see dashed lines in Fig. 5a). Obviously, the dimerisation of the ion radicals generated by the electrochemical oxidation occurs with the relatively short  $\pi$ -conjugated system<sup>13</sup> and therefore this band can be attributed to a dimerisation product. Very similar behaviour was observed in the oxidation of **15c** where the diphenylamino moiety of **15a** is replaced by a phenothiazinyl moiety. In this case, a very intense optical band at  $1.56 \text{ eV}$

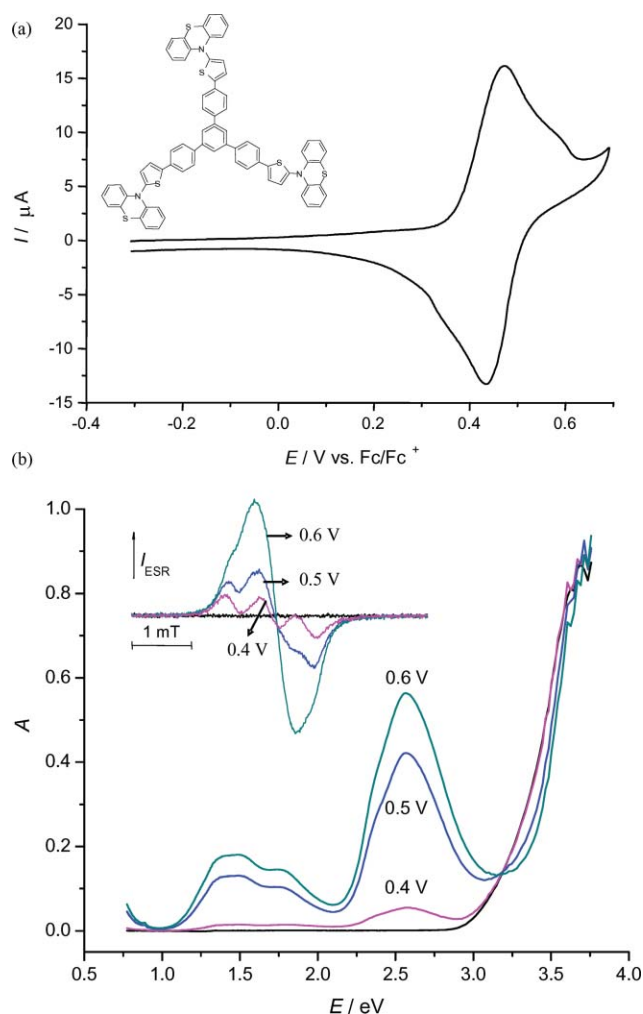


**Fig. 3** *In situ* ESR-UV/Vis/NIR spectroelectrochemistry of **16c** in  $\text{CH}_2\text{Cl}_2 + 0.2 \text{ mol L}^{-1} \text{ TBABF}_4$  at a platinum electrode. a) Cyclic voltammogram ( $\nu = 3 \text{ mV s}^{-1}$ , inset: structure of **16c**). b) UV/Vis/NIR spectra measured during a CV scan (inset: the corresponding ESR spectra measured at the marked potentials in volts vs.  $\text{Fc/Fc}^+$ ).

(795 nm), which corresponds to the follow-up reaction of the cation radical of **15c**, dominates the optical spectrum during anodic oxidation.

By incorporation of a thiophene moiety between the central benzene moiety and the diphenylamino-thiophene side fragments, resulting in compound **15b**, the extended structure results in the formation of stable charged states. Thus two well defined absorption maxima at 1.44 eV (694 nm) and 2.16 eV (574 nm) were found for the ion radicals generated from compound **15b** at the first oxidation peak. In contrast to **15a** for which an irreversible cyclic voltammetric response was measured *in situ* at a scan rate of  $3 \text{ mV s}^{-1}$  in an ESR flat cell, reversible behaviour was observed for **15b** at the same scan rate (Fig. 6). The ESR intensity of the cation radical **15b**<sup>+</sup> correlates well with the intensity of both optical bands in their potential dependence (Fig. 5b). During the voltammetric cycling an identical spectroelectrochemical response is observed for each cycle indicating that the incorporation of the thiophene moiety between the central moiety and its side

groups is an advantageous strategy to enhance the stability of charged states in the hole transporting starburst compounds. Subsequent dimerisation reactions of cation radicals of 2-diarylaminothiophene-based starburst compounds with short  $\pi$ -conjugation were eliminated by this strategy. Theoretical studies concerning the charge distribution and the intramolecular charge transfer within the newly prepared star-shaped molecules taking into account recent efforts in this field<sup>12,14</sup> are under way.

## Conclusion

We have demonstrated by an *in situ* spectroelectrochemical study the effects of structure on electrochemical and spectroelectrochemical behaviour of 2-diarylaminothiophene-based starburst compounds, which exhibit a high tendency to form amorphous glasses after cooling their melts. Four distinct reversible one-electron processes during oxidation of 2-diarylaminothiophene-based starburst compounds with the central triphenylamino moiety, **14**, were observed and the spin delocalisation on the central triphenylamino moiety in the monocation was confirmed. On the other hand the starburst compounds with the central 1,3,5-triphenylbenzene moiety, **16**, exhibit three strongly overlapping one-electron processes and the location of the spins on the core moieties was indicated at the first oxidation peak. The stability of the charged states was increased substantially by the incorporation of a thiophene moiety between the central moieties and the side groups for 2-diarylaminothiophene-based starburst compounds **15** with a central benzene moiety. This represents an advantageous strategy to enhance the stability of charge states in the hole transporting starburst compounds.

## Experimental

### General

The following instruments and analytical techniques were used. Melting points: Kofler hot-stage microscope, corrected; NMR: Inova 500 “max 2”. Varian 300 MHz spectrometer Gemini 300;  $\text{CDCl}_3$  was used as solvent; elemental analysis: LECO analyzer CHNS 932; MS: AMO spectrometer 402 (70 eV, EI); cyclic voltammetry: all cyclovoltammetric (CV) experiments were performed at room temperature with a PAR 273 potentiostat (EG&G, U.S.) in a glove-box (oxygen and water content below 1 ppm). A standard three-electrode arrangement with a platinum wire as a working electrode, a platinum coil as a counter electrode and a silver wire as a pseudo-reference electrode was used. Ferrocene (Fc) was added as the internal standard for a final voltammetric cycle and all potentials are referred to the  $\text{Fc/Fc}^+$  couple. The concentration of the samples ranges from  $5 \times 10^{-4}$  to  $1 \times 10^{-3} \text{ mol L}^{-1}$ ; spectroelectrochemistry: the ESR spectra were recorded using an EMX X-Band ESR spectrometer (Bruker, Germany) and the optical spectra by using a UV/Vis/NIR spectrometer system TIDAS (J&M, Aalen, Germany). Both the ESR spectrometer and UV-Vis-NIR spectrometer were triggered by a HEKA potentiostat PG 285 and the triggering was performed using software package PotPulse 8.53 (HEKA Electronic, Germany). As the supporting

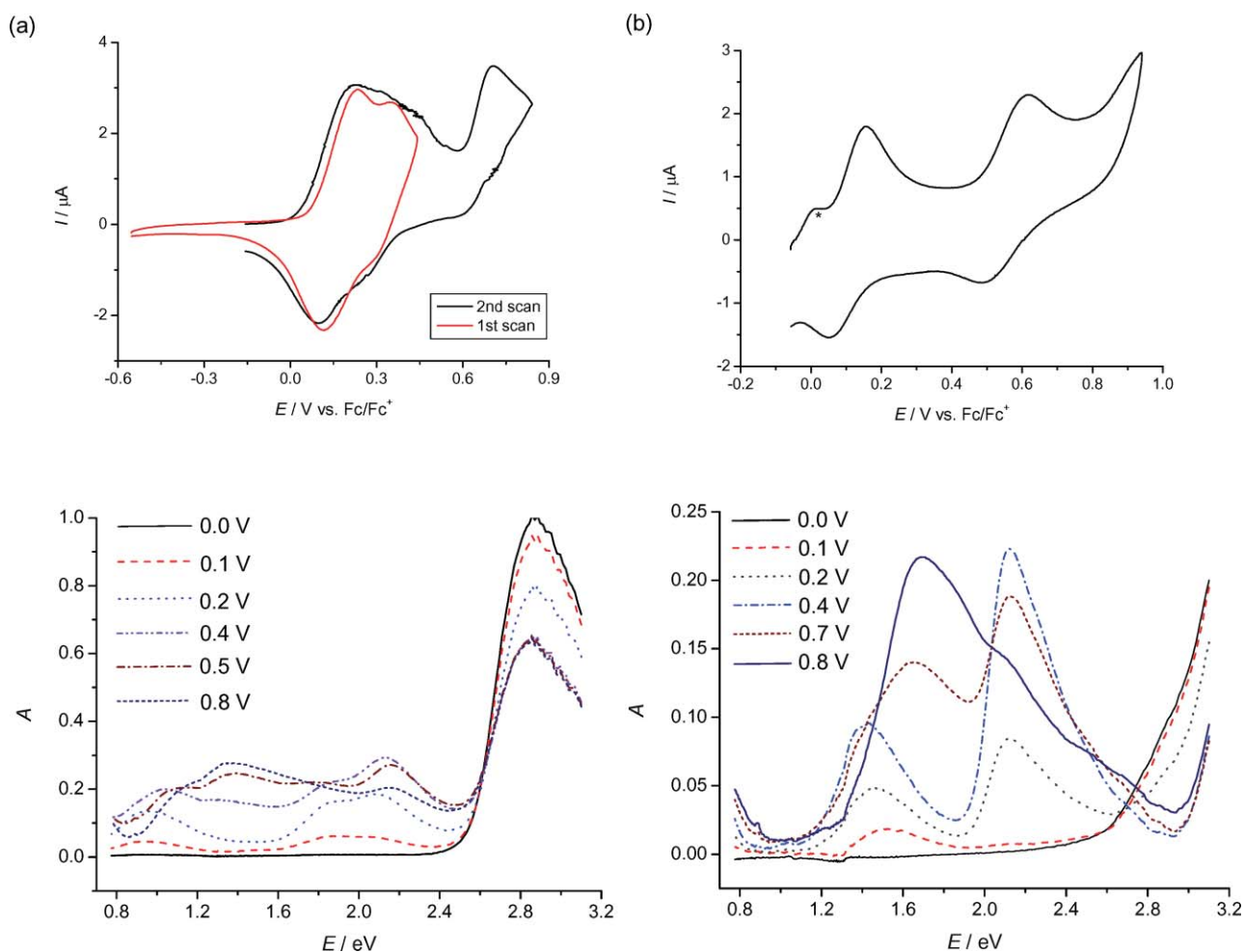


**Fig. 4** UV/Vis/NIR spectroelectrochemistry of (a) **14b** and (b) **16b** in  $\text{CH}_2\text{Cl}_2 + 0.2 \text{ mol L}^{-1}$  TBABF<sub>4</sub> (UV/VIS/NIR spectra taken in forward scan are shown for clarity; the potentials marked are in volts vs. Fc/Fc<sup>+</sup>; for **14b** UV/VIS/NIR spectra taken during the second cyclovoltammetric scan are shown in (a)).

electrolyte tetrabutylammonium tetrafluoroborate (TBABF<sub>4</sub>) was used, which was dried under reduced pressure at 340 K for 24 h and stored in a glove box prior to use. The concentration of TBABF<sub>4</sub> in dichloromethane ranges from 0.1 to 0.2 mol L<sup>-1</sup>.

## Materials

The 5-diaryl-amino-substituted thiophenes **5a** and **5b** as well as 5-diphenylamino-2,2'-bithiophene **5c** used as starting materials for the oxidative coupling reactions were prepared according to ref. 6.

## 2-Diarylaminothieryl-substituted starburst compounds 14–16 (general procedure)

(a) To a solution of a 2-diarylaminothiophene **5** (25 mmol) in absolute THF (310 mL) a solution (1.6 M) of BuLi in n-hexane (20 mL) was added dropwise under argon at  $-70^\circ\text{C}$ . After warming the reaction mixture to room temperature tributylstannyl chloride (10 mL, 0.1 M) was added. After standing of this mixture overnight it was poured into water (100 mL) and the product formed extracted by dichloromethane (100 mL).

The organic layer was dried with sodium sulfate, filtered, and evaporated *in vacuo*. The remaining product **9** was used without further purification for the next step.

(b) The tributylstannyl compound **10** (25 mmol) obtained was dissolved in absolute toluene (75 mL) and mixed under argon and under stirring, with an appropriate tribromoaryl compound **11**, **12**, or **13** (6 mmol) and Pd(PPh<sub>3</sub>)<sub>4</sub> (0.06 mmol, 0.07 g). After heating the resulting mixture was treated at  $80^\circ\text{C}$  for 8 h and the solvent was removed at reduced pressure. The residue was purified by column chromatography using silica as adsorbent and cyclohexane–toluene as eluent. The products **14–16** were thus obtained.

**4,4',4''-Tris(2-diphenylamino-5-thienyl)triphenylamine (14a).** From **5a** and **11** in a yield of 18% and a mp of  $90^\circ\text{C}$ . <sup>1</sup>H NMR (in CDCl<sub>3</sub>),  $\delta$  values (assignment): 6.69 (d,  $J = 4.2$  Hz, 3H), 7.02 (d,  $J = 8.7$  Hz, 6H), 7.07–7.11 (m, 18H), 7.22 (d,  $J = 3.9$  Hz, 3H), 7.29–7.35 (m, 12H), 7.49 (d,  $J = 8.1$  Hz, 6H). <sup>13</sup>C NMR (in CDCl<sub>3</sub>),  $\delta$  values: 121.6, 122.8, 123.2, 123.6, 125.2, 126.7, 129.8, 130.0, 138.8, 146.8, 148.4, 150.9. Calculated for C<sub>66</sub>H<sub>48</sub>N<sub>4</sub>S<sub>3</sub> (993.31) C, 79.80; H, 4.87; N, 5.64, S, 9.68; found C, 79.83; H, 4.81; N, 5.70; S, 9.60%. *m/z*: 993.

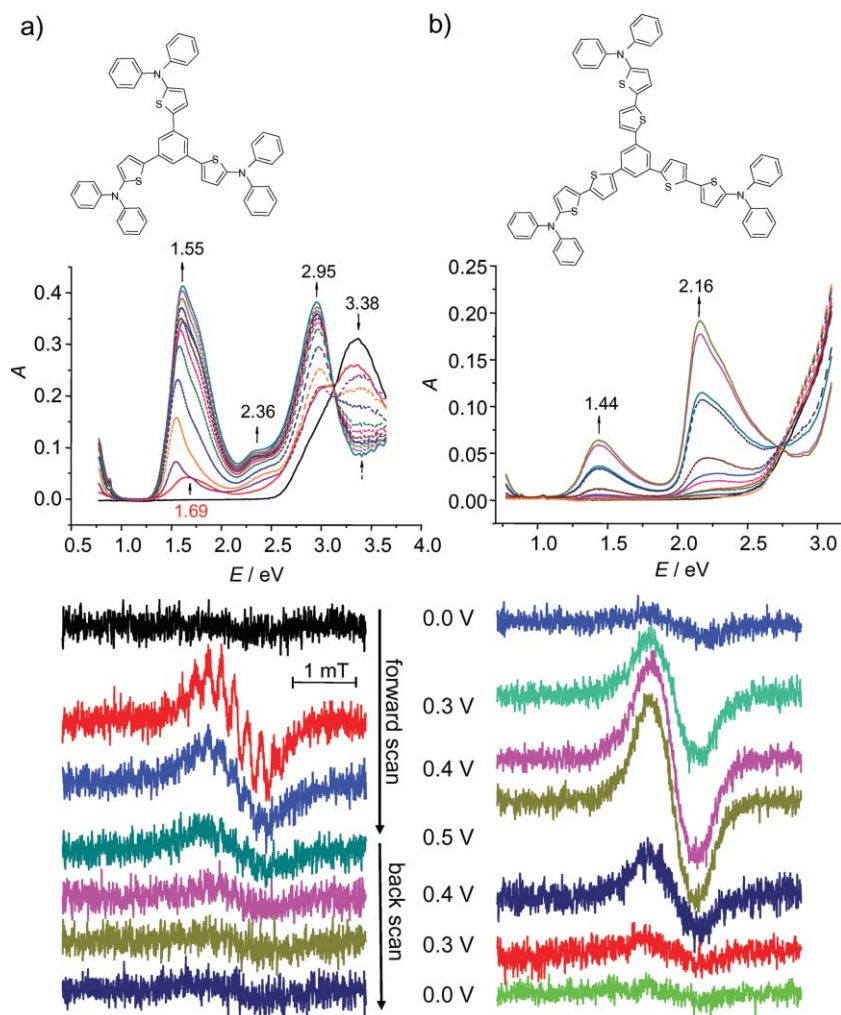


**Fig. 5** Spectroelectrochemistry of (a) **15a** and (b) **15b** in  $\text{CH}_2\text{Cl}_2 + 0.2 \text{ mol L}^{-1} \text{ TBABF}_4$  at a platinum mesh electrode in the potential range from  $-0.55 \text{ V}$  to  $0.45 \text{ V}$  vs.  $\text{Fc}/\text{Fc}^+$ . Identically colored ESR and optical (full lines - forward scan, dashed lines - back scan) spectra were taken at the same time during cyclic voltammetric scan ( $\nu = 3 \text{ mV s}^{-1}$ ). The potentials are marked in Volts vs.  $\text{Fc}/\text{Fc}^+$ .

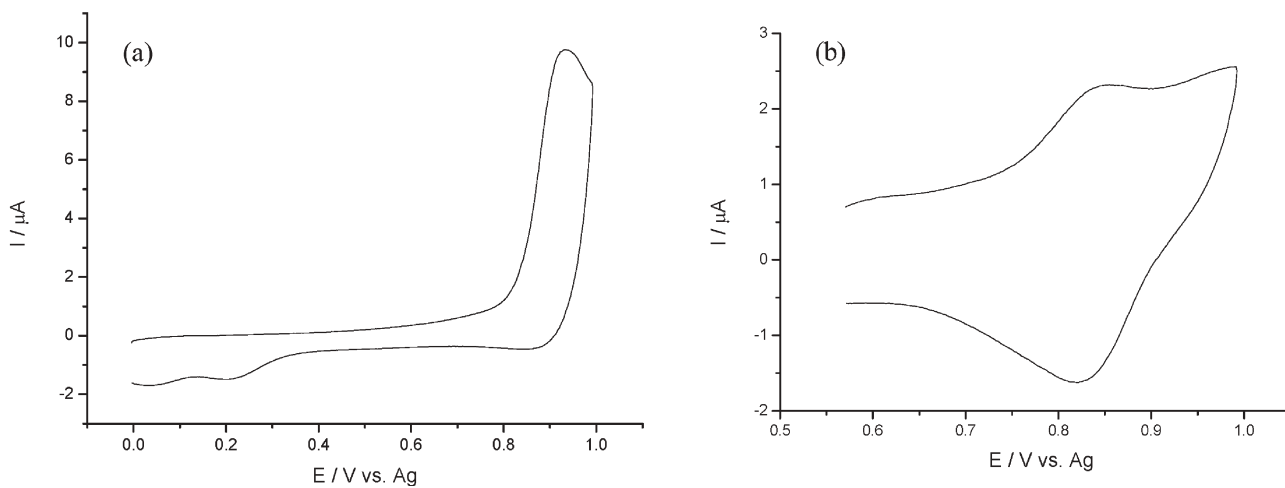


**Fig. 6** Cyclic voltammograms of (a) **15a** and (b) **15b** in  $\text{CH}_2\text{Cl}_2 + 0.2 \text{ mol L}^{-1} \text{ TBABF}_4$  at a platinum mesh electrode ( $\nu = 3 \text{ mV s}^{-1}$ ).

**4,4',4''-Tris(5'-diphenylamino-2,2'-bithien-5-yl)triphenylamine (14b).** From **5b** and **11** in a yield of 29% and a mp of 212 °C (decomp.). <sup>1</sup>H NMR (in CDCl<sub>3</sub>), δ values (assignment): 6.60 (d, *J* = 4.2 Hz, 3H), 6.96 (d, *J* = 3.9 Hz, 3H), 7.00 (d, *J* = 3.6 Hz, 3H), 7.03–7.08 (m, 6H), 7.11–7.14 (m, 9H), 7.17–7.21 (m, 12H), 7.27–7.31 (m, 12H) 7.47–7.50 (m, 6H). <sup>13</sup>C NMR (in CDCl<sub>3</sub>), δ values: 121.9, 122.7, 123.5, 123.8, 124.0, 124.4, 125.1, 127.2, 129.8, 129.9, 132.1, 137.3, 142.8, 147.1, 148.3, 151.2. Calculated for C<sub>78</sub>H<sub>54</sub>N<sub>4</sub>S<sub>6</sub> (1239.69) C, 75.57; H, 4.39; N, 4.52, S, 15.52; found C, 75.02; H, 4.91; N, 3.83; S, 15.03%. *m/z*: 1239.

**4,4',4''-Tris[5-(phenothiazin-10-yl)thien-2-yl]triphenylamine (14c).** From **5c** and **11** in a yield of 17% and a mp of 275 °C. <sup>1</sup>H NMR (in CDCl<sub>3</sub>), δ values (assignment): 6.80 (d, *J* = 4.2 Hz, 6H), 6.89 (t, *J* = 7.2 Hz, 6H), 6.98 (d, *J* = 7.5 Hz, 6H), 7.02–7.06 (m, 9H), 7.17 (d, *J* = 8.7 Hz, 6H), 7.30 (d, *J* = 3.9 Hz, 3H), 7.57 (d, *J* = 6.6 Hz, 6H). <sup>13</sup>C NMR (in CDCl<sub>3</sub>), δ values: 117.2, 12.6, 123.4, 124.8, 126.9, 127.4, 129.4, 129.7, 142.3, 143.6, 144.2, 147.1. Calculated for C<sub>66</sub>H<sub>42</sub>N<sub>4</sub>S<sub>6</sub> (1083.46) C, 73.16; H, 3.91; N, 5.17, S, 17.76; found C, 72.34; H, 4.06; N, 5.15; S, 17.14%. *m/z*: 1084.

**1,3,5-Tris[4-(2-diphenylamino-5-thienyl)phenyl]benzene (16a).** From **5a** and **13** in a yield of 16% and a mp of > 320 °C. <sup>1</sup>H NMR (in CDCl<sub>3</sub>), δ values (assignment): 6.69 (d, *J* = 3.9 Hz, 3H), 7.06 (t, *J* = 7.2 Hz, 6H), 7.17–7.30 (m, 27H), 7.65 (dd, *J* = 8.2 Hz, 12H), 7.78 (s, 3H). <sup>13</sup>C NMR (in CDCl<sub>3</sub>), δ values: 122.3, 122.5, 123.4, 123.8, 125.1, 126.2, 128.3, 129.8, 134.6, 138.1, 140.1, 142.4, 148.4, 151.9. Calculated for C<sub>72</sub>H<sub>51</sub>N<sub>3</sub>S<sub>3</sub> (1053.39) C, 82.02; H, 4.88; N, 3.99, S, 9.12; found C, 81.16; H, 4.88; N, 4.08; 8.99%. *m/z*: 1054.

**1,3,5-Tris[4-(5-phenothiazin-10-yl-2-thienyl)phenyl]benzene (16c).** From **5c** and **13** in a yield of 22% and a mp of 286 °C (decomp.). <sup>1</sup>H NMR (in CDCl<sub>3</sub>), δ values (assignment): 6.84 (d, *J* = 8.1 Hz, 6H), 6.91 (t, *J* = 7.52 Hz, 6H), 7.01 (t, *J* = 7.7 Hz, 6H), 7.06–7.09 (m, 9H), 7.40 (d, *J* = 3.9 Hz, 3H), 7.76 (m, 12H), 7.86 (s, 3H). <sup>13</sup>C NMR (in CDCl<sub>3</sub>), δ values: 117.8, 122.5, 122.7, 124.1, 125.56, 126.9, 127.5, 127.8, 128.6, 129.7, 134.3, 141.1, 142.5, 143.8, 143.9, 144.6. Calculated for C<sub>72</sub>H<sub>45</sub>N<sub>3</sub>S<sub>6</sub> (1144.54) C, 75.56; H, 3.96; N, 3.67, S, 16.81; found C, 75.47; H, 4.10; N, 3.71; S, 16.20%. *m/z*: 1145.

**1,3,5-Tris[4-(5'-diphenylamino-2,2'-bithien-5-yl)phenyl]benzene (16b).** from **5b** and **13** in a yield of 21% and a mp of 112 °C. <sup>1</sup>H NMR (in CDCl<sub>3</sub>), δ-values (assignment): 6.60 (d, *J* = 3.6 Hz, 6H), 6.99 (d, *J* = 3.9 Hz, 3H), 7.03–7.09 (m, 9H), 7.19–7.21 (m, 12H), 7.24–7.32 (m, 12H), 7.69 (s, 12H), 7.79 (s, 3H). <sup>13</sup>C NMR (in CDCl<sub>3</sub>), δ-values: 121.8, 122.9, 123.4, 123.9, 124.4, 124.5, 125.3, 126.6, 128.4, 129.9, 131.8, 134.1, 138.1, 140.5, 142.4, 142.5, 148.2, 151.4. Calculated for C<sub>84</sub>H<sub>57</sub>N<sub>3</sub>S<sub>6</sub> (1300.77) C, 77.56; H, 4.42; N, 3.23, S, 14.79; found C, 76.87; H, 4.43; N, 3.19; S, 14.17. *m/z*: 1301.

**1,3,5-Tris(5'-diphenylamino-2-thienyl)benzene (15a).** From **5a** and **12** in a yield of 17% and a mp of 209 °C. <sup>1</sup>H NMR (in CDCl<sub>3</sub>), δ values (assignment): 6.55 (d, *J* = 3.9 Hz, 3H),

7.04 (t, *J* = 7.2 Hz, 6H), 7.14 (d, *J* = 3.9 Hz, 3H), 7.18 (d, *J* = 7.2 Hz, 9H), 7.24–7.30 (m, 15H), 7.50 (s, 3H). <sup>13</sup>C NMR (in CDCl<sub>3</sub>), δ values: 120.6, 121.4, 122.3, 122.7, 123.1, 129.2, 135.6, 137.0, 147.6, 151.4. Calculated for C<sub>54</sub>H<sub>39</sub>N<sub>3</sub>S<sub>3</sub> (825.11) C, 78.51; H, 4.76; N, 5.09, S, 11.64; found C, 77.86; H, 5.15; N, 4.63; S, 11.53%. *m/z*: 825.

**1,3,5-Tris(5-phenothiazin-10-yl-2-thienyl)benzene (15c).** From **5c** and **12** in a yield of 18% and a mp of 245 °C. <sup>1</sup>H NMR (in CDCl<sub>3</sub>), δ values (assignment): 6.84 (d, *J* = 8.1 Hz, 6H), 6.91 (t, *J* = 7.5 Hz, 6H), 7.02 (t, *J* = 7.8 Hz, 6H), 7.08 (d, *J* = 6.6 Hz, 9H), 7.43 (d, *J* = 3.9 Hz, 3H), 7.78 (s, 3H). <sup>13</sup>C NMR (in CDCl<sub>3</sub>), δ values: 117.8, 122.6, 123.2, 123.5, 124.5, 127.5, 127.8, 129.3, 136.3, 142.7, 144.4, 144.5. Calculated for C<sub>54</sub>H<sub>33</sub>N<sub>3</sub>S<sub>6</sub> (916.26) C, 70.79; H, 3.63; N, 4.59, S, 21.00; found C, 69.95; H, 4.19; N, 4.40; S, 19.45%. *m/z*: 916.

**1,3,5-Tris(5'-diphenylamino-2,2'-bithien-5-yl)benzene (15b).** From **5b** and **12** in a yield of 25% and a mp of 108 °C. <sup>1</sup>H NMR (in CDCl<sub>3</sub>), δ values (assignment): 6.57 (d, *J* = 4.2 Hz, 3H), 6.97 (d, *J* = 3.9 Hz, 3H), 7.00–7.06 (m, 9H), 7.15–7.18 (m, 12H), 7.23–7.29 (m, 15H), 7.61 (s, 3H). <sup>13</sup>C NMR (in CDCl<sub>3</sub>), δ values: 121.5, 122.0, 123.0, 123.5, 124.0, 124.2, 125.0, 129.9, 131.5, 136.0, 138.5, 141.8, 148.2, 151.5. Calculated for C<sub>66</sub>H<sub>45</sub>N<sub>3</sub>S<sub>6</sub> (1072.48) C, 73.91; H, 4.23; N, 3.92, S, 17.94; found C, 73.93; H, 4.34; N, 3.83; S, 17.57%. *m/z*: 1072.

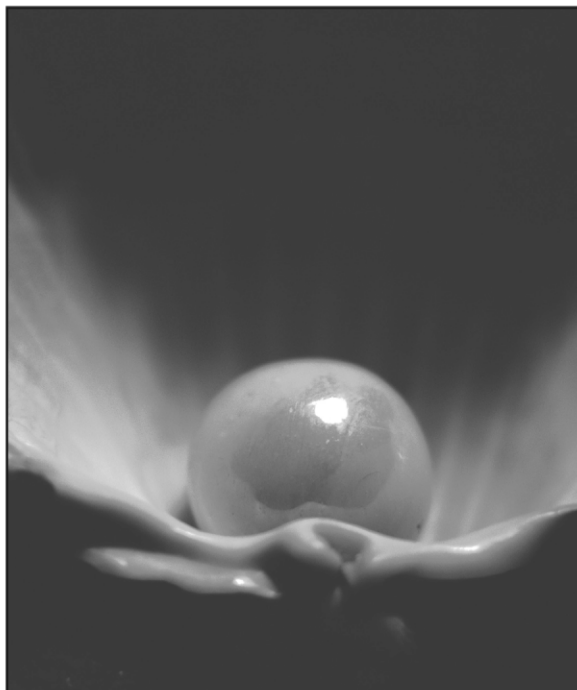
## Acknowledgements

Financial support by the Deutsche Forschungsgemeinschaft, by the Alexander von Humboldt Foundation (Projekt 3 Fokoop DEU/1063827) and the Slovak Scientific Grant Agency (1/3579/06) for P. R. is duly acknowledged.

## References

- T. Fuhrmann and J. Salbeck, *Adv. Photochem.*, 2002, **27**, 83–166; P. Strohrigl and J. V. Graulevicius, *Adv. Mater.*, 2002, **14**, 1439–1452.
- Handbook of Organic Conductive Molecules and Polymers*, ed. H. S. Nalwa, John Wiley, New York, 1997, vol. 1–4; Y. Shirota, *J. Mater. Chem.*, 2005, **15**, 75–93; Y. Shirota, *J. Mater. Chem.*, 2000, **10**, 1–25.
- J. F. Hartwig, *Angew. Chem.*, 1998, **110**, 2154–2174; J. F. Hartwig, *Angew. Chem., Int. Ed.*, 1998, **37**, 2047–2067; A. S. Guram, R. A. Rennels and S. L. Buchwald, *Angew. Chem.*, 1995, **107**, 1456–1458; A. S. Guram, R. A. Rennels and S. L. Buchwald, *Angew. Chem., Int. Ed. Engl.*, 1995, **34**, 1348–1350; E. Lukevics, P. Arsenyan and O. Pudova, *Heterocycles*, 2003, **60**, 663.
- H. Hartmann, P. Gerstner and D. Rohde, *Org. Lett.*, 2001, **3**, 1673–1675; D. Rohde, L. Dunsch, A. Tabet, H. Hartmann and J. Fabian, *J. Phys. Chem. B*, 2006, **110**, 8223–8231; P. Rapt, D. Rohde, H. Hartmann and L. Dunsch, *Tetrahedron Lett.*, 2006, **47**, 7587–7590.
- O. Zeika and H. Hartmann, *Tetrahedron*, 2004, **60**, 8213–8219; O. Zeika, H. Hartmann, K. Leo and M. Pfeiffer, DE 10343757, *Chem. Abstr.*, 2005, **142**, 411349.
- A. Tabet and H. Hartmann, *Synthesis*, 2005, 610–616.
- I.-Y. Wu, J. T. Lin, Y.-T. Tao, E. Balasubramaniam, Y. Z. Su and C.-W. Ko, *Chem. Mater.*, 2001, **13**, 2626–2631.
- I.-Y. Wu, J. T. Lin, Y.-T. Tao and E. Balasubramaniam, *Adv. Mater.*, 2000, **12**, 668–669; J. T. Lin, I.-Y. Wu, Y.-T. Tao and E. Balasubramaniam, *US Pat.* 2002115870, *Chem. Abstr.*, 2002, **137**, 185321.

- 9 A. Kanitz, J. Schumann, M. Scheffel, S. Rajoelson, W. Rogler, H. Hartmann and D. Rohde, *Chem. Lett.*, 2002, 896–897.
- 10 C. Heyde and I. Zug. H. Hartmann, *Eur. J. Org. Chem.*, 2000, 3273–3278.
- 11 S. Liu, K. S. Lin, V. M. Churikov, Y. Z. Su, J. T. Lin, T. H. Huang and C. C. Hsu, *Chem. Phys. Lett.*, 2004, **390**, 433–439.
- 12 Y. Hirao, A. Ito and K. Tanaka, *J. Phys. Chem. A*, 2007, **111**, 2951–2956; Y. Hirao, H. Ino, A. Ito and K. Tanaka, *J. Phys. Chem. A*, 2006, **110**, 4866–4872.
- 13 P. Rapta, N. Schulte, A.-D. Schlüter and L. Dunsch, *Chem.–Eur. J.*, 2006, **12**, 3103–3113 and references cited therein.
- 14 S. Amthor, C. Lambert, S. Dümmler, I. Fischer and J. Schelter, *J. Phys. Chem. A*, 2006, **110**, 5204–5214.



## Looking for that **special** chemical biology research paper?

TRY this free news service:

### Chemical Biology

- highlights of newsworthy and significant advances in chemical biology from across RSC journals
- free online access
- updated daily
- free access to the original research paper from every online article
- also available as a free print supplement in selected RSC journals.\*

\*A separately issued print subscription is also available.

Registered Charity Number: 207890

RSCPublishing

[www.rsc.org/chembiology](http://www.rsc.org/chembiology)

20030681